Increased Metallothionein I/II Expression in Patients with Temporal Lobe Epilepsy

PLOS ONE, SAN FRANCISCO, v. 7, n. 9, supl. 4, Part 1-2, pp. 541-545, SEP 18, 2012
http://www.producao.usp.br/handle/BDPI/35023

OPEN ACCESS Freely available online

PLOS ONE

Increased Metallothionein I/II Expression in Patients with Temporal Lobe Epilepsy

José Eduardo Peixoto-Santos[1], Orfa Yineth Galvis-Alonso[4], Tonicarlo Rodrigues Velasco[1], Ludmyla Kandratavicius[1], João Alberto Assirati[2], Carlos Gilberto Carlotti[2], Renata Caldo Scandiuzzi[1], Luciano Neder Serafini[3], João Pereira Leite[1]*

1 Department of Neuroscience and Behavior, Ribeirão Preto School of Medicine, University of São Paulo, Ribeirão Preto – São Paulo, Brazil, **2** Department of Neurosurgery, Ribeirão Preto School of Medicine, University of São Paulo, Ribeirão Preto – São Paulo, Brazil, **3** Department of Pathology, Ribeirão Preto School of Medicine, University of São Paulo, Ribeirão Preto – São Paulo, Brazil, **4** Department of Molecular Biology, São José do Rio Preto Medical School, São José do Rio Preto – São Paulo, Brazil

Abstract

In the central nervous system, zinc is released along with glutamate during neurotransmission and, in excess, can promote neuronal death. Experimental studies have shown that metallothioneins I/II (MT-I/II), which chelate free zinc, can affect seizures and reduce neuronal death after *status epilepticus*. Our aim was to evaluate the expression of MT-I/II in the hippocampus of patients with temporal lobe epilepsy (TLE). Hippocampi from patients with pharmacoresistant mesial temporal lobe epilepsy (MTLE) and patients with TLE associated with tumor or dysplasia (TLE-TD) were evaluated for expression of MT-I/II, for the vesicular zinc levels, and for neuronal, astroglial, and microglial populations. Compared to control cases, MTLE group displayed widespread increase in MT-I/II expression, astrogliosis, microgliosis and reduced neuronal population. In TLE-TD, the same changes were observed, except that were mainly confined to *fascia dentata*. Increased vesicular zinc was observed only in the inner molecular layer of MTLE patients, when compared to control cases. Correlation and linear regression analyses indicated an association between increased MT-I/II and increased astrogliosis in TLE. MT-I/II levels did not correlate with any clinical variables, but MTLE patients with secondary generalized seizures (SGS) had less MT-I/II than MTLE patients without SGS. In conclusion, MT-I/II expression was increased in hippocampi from TLE patients and our data suggest that it is associated with astrogliosis and may be associated with different seizure spread patterns.

Citation: Peixoto-Santos JE, Galvis-Alonso OY, Velasco TR, Kandratavicius L, Assirati JA, et al. (2012) Increased Metallothionein I/II Expression in Patients with Temporal Lobe Epilepsy. PLoS ONE 7(9): e44709. doi:10.1371/journal.pone.0044709

Editor: Stefano L. Sensi, University G. D'Annunzio, Italy

Received June 17, 2012; **Accepted** August 7, 2012; **Published** September 18, 2012

Funding: The present work was supported by Fundação de Amparo à Pesquisa do Estado de São Paulo (FAPESP, research grants 2005/56447-7 and 2009/53447-7 to JPL and master's grant 2008/52657-5 to JEPS), Conselho Nacional de Desenvolvimento Científico e Tecnológico (CNPq) and Coordenação de Aperfeiçoamento de Pessoal de Nível Superior (CAPES). The funders had no role in study design, data collection and analysis, decision to publish, or preparation of the manuscript.

Competing Interests: The authors have declared that no competing interests exist.

* E-mail: jpleite@fmrp.usp.br

Introduction

Zinc (Zn^{2+}) is an important modulator of glutamatergic transmission in the central nervous system (CNS) [1], [2], [3]. Zn^{2+} is concentrated in presynaptic vesicles, along with glutamate, and released during normal neurotransmission [4], [5], [6], [7], [8]. Hippocampal neurons are specially rich in vesicular Zn^{2+}, particularly in the axonal boutons of granule cells, CA3 and CA1 pyramidal cells and prosubicular neurons [5], [6], [7], [9], [10]. In temporal lobe epilepsy (TLE), one of the most frequent drug-resistant epilepsies in adults, the hippocampus is associated with seizure generation [11], [12]. The intense neuronal activity during seizures can induce high amounts of Zn^{2+} in the synaptic cleft, [13], [14] promoting reactive oxygen species (ROS) production, [15] which can ultimately lead to hippocampal neuronal death [16], [17], [14], [15], [13]. In fact, studies in hippocampi from TLE patients who underwent epilepsy surgery have shown neuronal loss [18], [19], [20], increased glial reaction [21], [22], [23], [24] and reorganization of mossy fibers axon collaterals into the inner molecular layer of the granule cell dendrites [25], [19]. This synaptic reorganization of Zn^{2+}-enriched terminals has been hypothesized to contribute to synchronous firing and epileptiform activity [19]. Besides the vesicular Zn^{2+}, other intracellular Zn^{2+} pools are present in neurons [26], [27], which can also contribute to neuronal death after an insult [28], [29], [27].

Metallothioneins (MTs) are low molecular weight, cystein-enriched proteins that bound Zn^{2+} and cadmium. They can be found in various tissues, in four isoforms [30]. Isoforms I, II and III are found in the central nervous system (CNS), where the isoforms I and II are expressed in astrocytes and the isoform III is expressed only in neurons [31], [32]. MTs participate in Zn^{2+} homeostasis, scavenging ROS in the brain [33] and stimulate the expression of several neurotrophic and antiinflamatory factors [34]. Studies on rodent models of TLE have shown that MT expression is increased in the hippocampal formation shortly after seizures [35], [36] and that high levels of MTs I and II are associated with reduced neuronal death after seizure-induced damage [37], [36], [38]. However, some studies with neuronal MT (MT-III) indicate that MTs could also contribute to neuronal death in some circumstances [39], [29].

Since MT-I/II levels may be associated with neuron survival after seizures, we hypothesize that MT-I/II expression is altered in TLE and can be associated with the preservation of neuronal density in the hippocampus of TLE patients. Therefore, in this study we evaluated the immunoexpression of MT-I/II and its correlation with hippocampal neuron density in hippocampi of patients with chronic TLE.

Materials and Methods

Patients and clinical data

Patients with drug-resistant epilepsy were evaluated at the University of São Paulo Epilepsy Surgical Centre in Ribeirão Preto (Brazil), according to standard protocols published elsewhere [40]. The presurgical evaluation protocol included interviews for epilepsy history, neurological examination, EEG recording, video-EEG assessment, T1- and T2-weighted MRI, ictal and interictal single-photon emission computed tomography (SPECT) scans and neuropsychological tests. Drug resistance was defined according to previous published literature [41].

TLE patients were divided in two groups: (i) mesial TLE (MTLE) and (ii) TLE associated with extrahippocampal tumor or dysplasia (TLE-TD). MTLE group (n = 69) were patients with hippocampal atrophy or with normal hippocampal volume at MRI without other lesions associated with TLE. TLE-TD (n = 17) were TLE patients with tumor or cortical dysplasia in temporal lobe structures other than the hippocampus. From all TLE-TD patients, 4 had non-Taylor focal cortical dysplasia and the remaining had tumors. The tumors observed were grade I ganglioglioma (n = 3), grade I dysembryoplastic neuroepithelial tumor (n = 3), hamartoma (n = 3), teratoma (n = 2), grade III astrocytoma (n = 1) and angioma (n = 1).

For comparison purposes in the neuropathology studies, autopsy controls (Ctrl, n = 19) were obtained from autopsy cases without history of neurological diseases, with no sign of CNS pathologies in *post mortem* pathological evaluation and no history of hypoxic episodes during agony. *Post mortem* time (i.e., time between death and hippocampal fixation) was of 5.15±1.43 hours, ranging from 3.16 to 9 hours. The causes of death were pulmonary insuficiency (n = 6), cardiomyopathy (n = 3), cardiogenic shock (n = 2), sepsis (n = 3), hepatic failure (n = 3), acute lymphoblastic leukemia (n = 1) and gastric adenocarcinoma (n = 1).

Medical records of all evaluated patients were assessed for clinical data analysis. The clinical variables investigated were age at death and cause of death for Ctrl patients and age at surgery, epilepsy duration, age at the first recurrent seizure, seizure frequency per month, presence of secondary generalized seizures, and neuropathological evaluation for TLE patients. This study followed the principles of the Declaration of Helsinki, was registered in Brazilian's Health Ministry and was approved by the Research Ethics Committee of the Hospital das Clínicas, where this study was performed (process HCRP 2634/2008). Written informed consent was obtained from all patients used in this study, and the Research Ethics Committee also approved the Consent Term. Tissue from autopsy cases came from a Brain Bank approved by the Research Ethics Committee of Hospital das Clínicas (process HCRP 9370/2003).

Tissue collection and histological techniques

Hippocampi from surgery or autopsy were cut in coronal sections and placed in 10% (vol/vol) buffered formaldehyde for one week, followed by paraffin embedding. Immunohistochemistry was performed in 8 μm sections at the level of hippocampal body for evaluation of neuronal, astroglial and activated microglial populations and for MT-I/II expression with antibodies against, respectively, NeuN, GFAP, HLA-DR and MT-I/II. The sections were submitted to endogenous peroxidase blocking with 4.5% H_2O_2 in 50 mM phosphate-saline buffer (PSB) pH 7.4, for 15 minutes, followed by microwave antigenic retrieval in 10 mM sodium citrate buffer pH 6.0 (for GFAP) or 50 mM Tris-HCl pH 9.6 (for NeuN, HLA-DR and MT-I/II). After achieving room temperature, the sections went through blocking free aldehyde groups with Tris-glycine 0.1 M pH 7.4 for 45 minutes, followed by blocking buffer with 5% defatted milk and 15% goat serum (#S-1000, Vector) in Triton buffer (PTB, 20 mM phosphate +0.45 M NaCl, pH 7.4, with 0.3% Triton X-100) for four hours. The sections were then incubated with primary antibodies in blocking buffer for 16 hours. We used primary monoclonal antibodies raised in mouse anti-human GFAP (clone 6F2, #M0761, Dako), anti-murine NeuN (clone A60, #MAB377, Chemicon), anti-human HLA-DR (clone TAL.1B5, #M0746, Dako) and anti-equine MT-I/II (clone E9, #M0639, Dako), diluted in blocking buffer at concentrations of 1:500, 1:500, 1:100 and 1:500, respectively. The primary antibodies were detected using biotinylated rabbit anti-murine IgG (#E0354, Dako), at 1:200 dilution in blocking buffer, for one hour, followed by revelation with avidin-biotin-peroxidase system (Vectastain Elite ABC kit, #PK6100, Vector) and diaminobenzidine as chromogen (DAB, #34001, Pierce Biotechnology). The development times in DAB solution were 12 minutes for HLA-DR, 10.5 minutes for NeuN and 8 minutes for MT-I/II and GFAP. In order to assure that the different times of fixation of autopsy hippocampi and surgical tissue were comparable, an additional experiment was performed with temporal cortical tissue from one TLE patient. Briefly, a cortical sample was removed during surgery, sectioned in 5 fragments which were kept at room temperature for 1, 2, 4, 6 and 8 hours before immersion-fixation in 10% buffered formaldehyde. Sections of these cortical fragments with different pre-fixation times were mounted on slides and processed in the same manner as the surgical and autopsy hippocampi.

Vesicular Zn^{2+} was evaluated in a subset of cases by neo-Timm histochemistry [19]. Briefly, a fresh hippocampal section was placed in buffered fixative solution (4% glutaraldehyde and 0.1% sodium sulfite) at 4°C for one week, followed by water removal with 20% buffered saccarose for one day. The fragment was dried and frozen in cryostat. Thirty μm sections were utilized for neo-Timm technique, according to previously published protocols [19], [42], [43].

Immunofluorescence

Colocalization of MT-I/II with neuronal and astroglial markers was performed with the same protocol described above. Endogenous peroxidase blocking and the revelation procedure were omitted. Primary antibodies were raised in mouse anti-equine for MT-I/II (clone E9, #M0639, Dako), in rabbit anti-cow for GFAP (#Z0334, Dako) and anti-human for MAP2 (#sc-20172, Santa Cruz Biotechnology). Sections were submitted to MT-I/II plus GFAP or MT-I/II plus MAP2 incubation, with antibodies diluted in blocking buffer at 1:100 for MT-I/II, 1:1000 for GFAP and 1:50 for MAP2, for 20 hours. The primary antibodies were detected using goat anti-mouse IgG conjugated with Alexa Fluor 488 (#A11001, Molecular Probes) and goat anti-rabbit IgG conjugated with Texas Red (#T2767, Molecular Probes), diluted in blocking buffer, at 1:300 each, for 2 hours. Following incubation, the sections were submitted to Hoechst 33342 staining (#H1399, Molecular Probes) for 4 minutes, and were mounted in Fluoromount-G (#17984-25, EMS). With this procedure, GFAP and MAP2 were observed in red, MT-I/II in green and cell

nucleus in blue. All images were captured in Leica SP5 confocal microscope.

Histological analysis

Images of all hippocampal regions were obtained with a video monochrome charge-coupled device camera (CCD; Hamamatsu Photonics Model 2400, Japan) attached to an Olympus microscope (Model BX60, Melville, NY), and captured, averaged, and digitized using a frame grabber (Scion Corporation, Frederick, MD) on a Macintosh computer (Model G3, Cupertino, CA). Illumination exposure was uniformly maintained and regularly checked using optical density standards (Kodak, Rochester, NY) in order to prevent any distortion of measurements (immunopositive area, gray level) between the samples. After captured, the image was analyzed using image system software (ImageJ, version 1.37c).

Quantification of the immunohistochemistry was performed with threshold tool, with the investigator blind to the group allocation. After the selection of the region of interest (ROI), the software calculated the immunopositive area by counting all pixels with gray intensity equal or superior to the threshold of staining. A complete protocol for threshold tool can be found at rsbweb.nih.gov/ij/docs/examples/stained-sections/index.html. The threshold was defined for each protein evaluated, based on the mean immunopositivity of all control cases. The evaluated regions were the *fascia dentata* (outer molecular layer, inner molecular layer, granule cell layer, subgranular zone), the hilus and the stratus piramidale of CA4, CA3, CA2, CA1, prosubiculum and subiculum (**Figure 1**). The characterization of hippocampal regions was based on the Lorente de Nó's classification [44]. Results were shown as percentage of immunopositive area/total area.

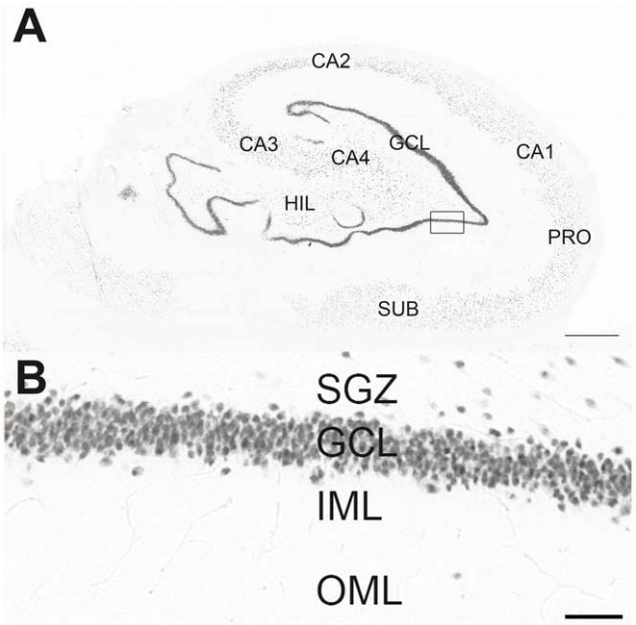

Figure 1. Subfields in the hippocampal formation under NeuN immunohistochemistry. In A can be seen: the granule cell layer of *fascia dentata* (GCL, composed by granular neurons) and the hilus (HIL, composed by several types of interneurons); pyramidal neuronal layers of the hippocampus (CA4-CA1); the subicular formation, composed by prosubiculum (PRO) and subiculum (SUB). In B, a higher magnification of the fascia dentate (marked as a black square in A), composed by subgranule zone (SGZ), granule cell layer (GCL), inner molecular layer (IML) and outer molecular layer (OML). Bar in A indicates 1 millimeter and in B indicates 50 micrometers.
doi:10.1371/journal.pone.0044709.g001

Additionally, neuronal density was evaluated in the NeuN stained sections. Neuronal count was processed in ImageJ 1.37c software with a 520× magnification for granule cell layer and 260× for pyramidal neurons of CA4, CA3, CA2, CA1, prosubiculum and subiculum. Neuronal densities were estimated with the correction of Abercrombie [45], which permits to estimate the neuronal density through mathematical method, and the results were shown as thousands of cells per cubic millimeter.

Quantification of neo-Timm sections was done by measurement of mean gray value, which varied from 0 to 255, of the hippocampal regions in ImageJ software. The evaluated regions comprised outer molecular layer, inner molecular layer, granule cell layer, subgranule zone and hilus/CA4.

Statistical analysis

Statistics were carried out in SigmaStat 3.1 software for all tests except for simple regression models, which were performed with SPSS 20. Tests for normality and homogeneity of variances were performed to define data distribution. For parametric variables, One Way ANOVA with Bonferroni *post hoc* or t-test was performed. For the non-parametric variables, Kruskal-Wallis with Dunn *post hoc* or Mann-Whitney tests were used. Fisher's exact test was performed to evaluate categorical data. Correlation between MT expression and cellular populations was performed using the Spearman's test, when $n \leq 30$, or Pearson's test, for $n > 30$. Multiple linear regressions were used to define associations between age, neuronal and astroglial populations over MT-I/II expression. All results were considered significant at $p < 0.05$.

Results

Clinical data

The clinical characteristics of study participants are summarized in Table 1. The mean age at evaluation was significantly lower in TLE-TD group than Ctrl and MTLE groups (Kruskal-Wallis, $p = 0.001$). Epilepsy duration was lower in TLE-TD group than in MTLE group (Mann-Whitney, $p = 0.002$). Recurrent seizures onset (t-test, $p = 0.651$), minimal seizure frequency in a month (Mann-Whitney, $p = 0.397$) and frequency of secondary generalized seizures per month (Mann-Whitney, $p = 0.557$) were similar in MTLE and TLE-TD groups. Fisher's exact test showed that the prevalence of secondary generalized seizures was similar between MTLE and TLE-TD ($p = 1.0$).

Changes in immunoreactivity in different fixation times

Quantification of MT-I/II, NeuN, GFAP and HLA-DR immunostaining in sections of cortical fragment in different fixation times revealed that a delay on fixation time was not associated with a decrease of immunoreactivity for all antibodies evaluated (**Figure S1**).

Neuronal density

NeuN immunopositive cells (**Figure 2**) were counted to estimate the neuronal density in the hippocampal subfields. The quantification studies (**Figure 3**) revealed reduced neuronal density in granule cell layer (Kruskal-Wallis, $p < 0.001$), CA4 (Kruskal-Wallis, $p < 0.001$), CA1 (Kruskal-Wallis, $p < 0.001$) and prosubiculum (ANOVA, $p < 0.001$) of the MTLE group, when compared to Ctrl and TLE-TD groups. In CA2 subfield, the neuronal densities of MTLE and TLE-TD groups were reduced when compared to Ctrl (ANOVA, $p < 0.001$). In CA3, MTLE and TLE-TD had reduced neuronal density when compare to each other and to the Ctrl group (ANOVA, $p < 0.001$). No differences in

Table 1. Clinical history of patients with TLE (MTLE and TLE-TD) and Ctrl cases.

Group	Ctrl	MTLE	TLE-TD	P value
Age at evaluation[1] (years)	42±16[#]	38±10[#]	26±12	0. 001
Epilepsy duration (years)	____	25±10[#]	15±12	0.002
Age at epilepsy onset (years)	____	13±9	12±7	0.651
Minimal seizure frequency (per month)	____	16±23	25±36	0.397
Number of secondary generalizations (per month)	____	4±7	4±9	0.557
Frequency of secondary generalization (%)	____	59	63	1.000

[1]age of death for Ctrl and age at surgery for TLE.
[#] = statistical difference to TLE-TD; Ctrl = control; MTLE = mesial temporal lobe epilepsy; TLE-TD = temporal lobe epilepsy associated with tumor or dysplasia.
doi:10.1371/journal.pone.0044709.t001

neuronal density were found in the subiculum (ANOVA, $p = 0.08$). All hippocampal regions of MTLE group showed reduced NeuN immunopositive area when compared with Ctrl, in agreement with neuron density measurements (Data not shown).

Vesicular Zn^{2+} evaluation

Vesicular Zn^{2+} content (**Figures 2** and **4**), estimated by gray value of neo-Timm staining, was increased only in the inner molecular layer of MTLE patients, compared to Ctrl ($p<0.001$). No differences were observed between Ctrl, MTLE and TLE-TD in the outer molecular layer ($p = 0.275$), granule cell layer ($p = 0.196$), subgranule zone ($p = 0.467$) or hilus/CA4 ($p = 0.843$).

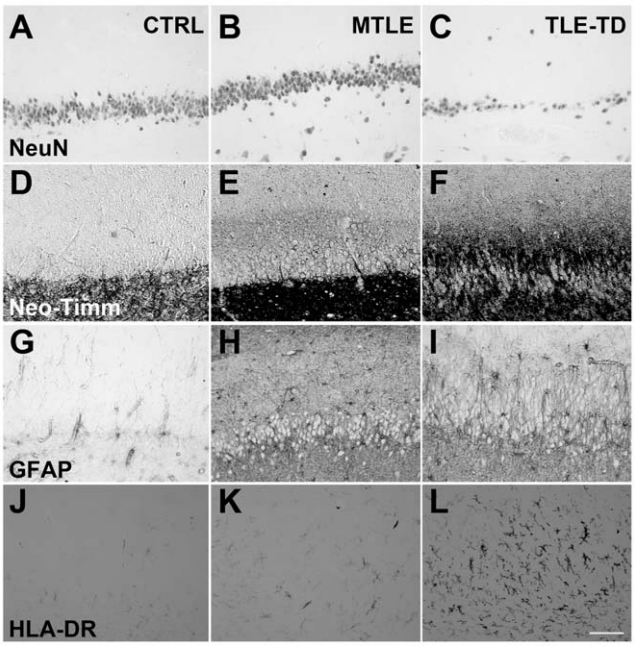

Figure 2. Representative images of NeuN, neo-Timm, GFAP and HLA-DR staining in the *Fascia dentata* of Ctrl, TLE-TD and MTLE patients. The pattern of NeuN staining is the same in Ctrl (A), TLE-TD (B) and MTLE (C) groups, but MTLE shows reduced neuronal population in this subfield. Compared to Ctrl (D), increased neo-Timm staining was observed in the inner molecular layer of *fascia dentata* in MTLE patients (F), but not in TLE-TD (E). As for the astroglial population, both hyperplasia and hypertrophy are observed in MTLE (I) and TLE-TD (H), compared to Ctrl (G). Hyperplasia is also observed in microglial cells in TLE-TD (K) and, more notable, in MTLE (L), compared to Ctrl (J). Bar in L indicates 100 micrometers.
doi:10.1371/journal.pone.0044709.g002

Reactive astroglial population

GFAP immunopositive area, shown in **Figures 2** and **5**, indicated increased GFAP immnunoreactivity labeling in the outer and inner molecular layers, granule cell layer, subgranule zone, hilus and CA4 of MTLE and TLE-TD, when compared to Ctrl (ANOVA for granule cell layer and Kruskal-Wallis for the remaining regions, $p<0.001$). In CA2, Sommer sector (CA1 and prosubiculum) and the subiculum, there was increased GFAP immnunoreactivity labeling of the MTLE group, when compared to Ctrl and TLE-TD (Kruskal-Wallis, $p<0.001$). Increased reactive astrogliosis was also observed in CA3 of MTLE (Kruskal-Wallis, $p<0.001$), when compared to Ctrl.

Activated microglial population

HLA-DR immunopositive area, shown in **Figures 2** and **6**, indicated increased labeling in subgranule zone (Kruskal-Wallis, $p = 0.002$), hilus (Kruskal-Wallis, $p = 0.017$), CA3 (Kruskal-Wallis, $p<0.001$), CA2 (Kruskal-Wallis, $p<0.001$), prosubiculum (Kruskal-Wallis, $p<0.001$) and subiculum (Kruskal-Wallis, $p = 0.009$) of MTLE group, when compared to Ctrl. In outer molecular layer, granule cell layer and CA4 (Kruskal-Wallis, $p<0.001$) HLA-DR immunopositivity was increased in MTLE and TLE-TD groups, when compared to Ctrl. MTLE group showed increased staining in the inner molecular layer and CA1 when compared to both TLE-TD and Ctrl groups (Kruskal-Wallis, $p<0.001$).

Metallothionein I/II immunoreactivity

MT-I/II staining revealed both cellular and neuropil staining (**Figure 7A–F**). MT-I/II-positive cells had astrocyte morphology, with small round soma and radial processes (**Figure 7A–D**). The staining was present in nucleus, cytoplasm and the proximal portion of the cytoplasmic processes. In two individuals of the Ctrl group and in one MTLE patient, some cells with neuronal morphology and size were also stained for MT-I/II (**Figure 7E, F**). No microglia-like cells were stained for MT-I/II. Neuropil staining showed a granular pattern in all hippocampal subfields (**Figure 7A–F**). Confocal microscopy confirmed the expression of MT-I/II in astrocytes by GFAP-positive labeling (**Figure 8**). A comparison between MT-I/II expression in Ctrl, TLE-TD and MTLE groups is shown in **Figure 9**.

Higher MT-I/II immunoreactivity area (**Figure 10**) was observed in both TLE groups, when compared to Ctrl group. The increase in MT-I/II immunoreactivity area observed in TLE was due to an increased number of MT-I/II-positive cells and to increased neuropil staining. MTLE group showed increased immunopositive area when compared to Ctrl in granule cell layer (Kruskal-Wallis, $p = 0.028$), hilus (Kruskal-Wallis, $p<0.001$), CA3

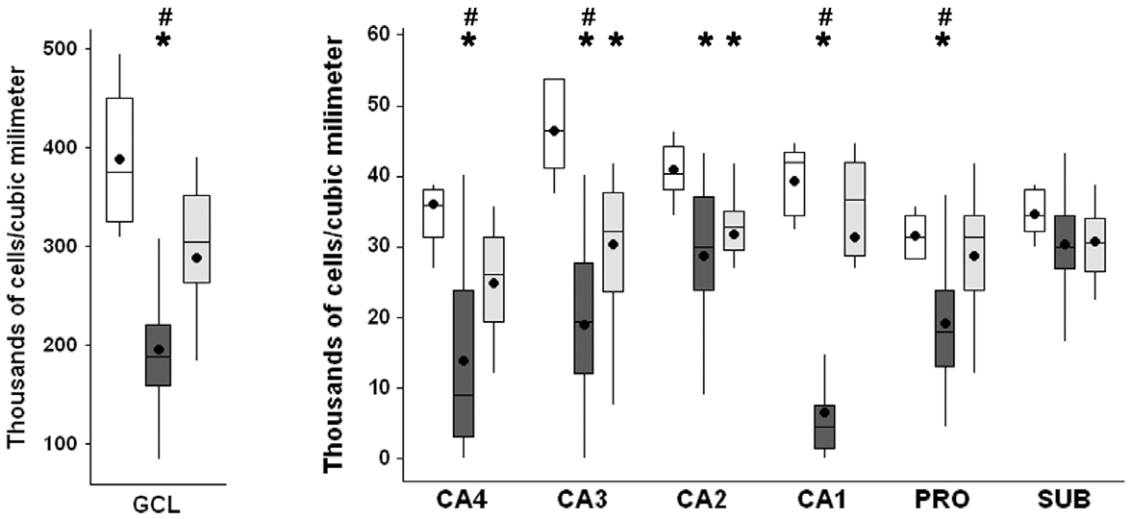

Figure 3. Neuronal density in hippocampal subfields of Ctrl, MTLE and TLE-TD groups. MTLE (dark gray boxplots) had reduced neuronal density (showed as thousands of cells per cubic millimeter), when compared to Ctrl (white boxplots) and TLE-TD (light gray boxplots), in granule cell layer (GCL), CA4, CA3, CA1 and prosubiculum, and in CA2, when compared to Ctrl ($p<0.001$). TLE-TD presented decreased neuronal density only in CA3 and CA2, compared to Ctrl ($p<0.001$). The * indicate difference from Ctrl and # difference from TLE-TD. The dark circles indicate mean.
doi:10.1371/journal.pone.0044709.g003

(ANOVA, $p = 0.003$), CA2 (Kruskal-Wallis, $p<0.001$) and subiculum (Kruskal-Wallis, $p<0.001$) and in CA4 when compared to TLE-TD (Kruskal-Wallis, $p = 0.041$). Both MTLE and TLE-TD groups had increased MT-I/II immunopositive area when compared to Ctrl in outer molecular layer (Kruskal-Wallis, $p = 0.002$), inner molecular layer (Kruskal-Wallis, $p = 0.023$), and subgranule zone (Kruskal-Wallis, $p<0.001$). In CA1 and the prossubiculum, the immunopositive area was increased in MTLE when compared with both TLE-TD and Ctrl (ANOVA, $p<0.001$).

MT-I/II immunoreactivity and seizures

In MTLE group, patients without secondary generalized seizures (SGS) had increased MT-I/II immunopositivity, when compared with patients with SGS, in the inner molecular layer (t-test, $p = 0.037$), granule cell layer (t-test, $p = 0.018$), subgranule zone (t-test, $p = 0.004$), CA2 (Mann-Whitney, $p = 0.039$) and CA1 (t-test, $p = 0.043$) (**Figure 11**). No differences in neuronal, astroglial or microglial populations were observed between MTLE patients with or without SGS. In TLE-TD patients, no differences in hippocampal MT-I/II immunopositivity, neuronal, astroglial or microglial populations were observed between patients with and without SGS. Frequency of seizures did not correlate with MT-I/II immunopositivity in all hippocampal subfields.

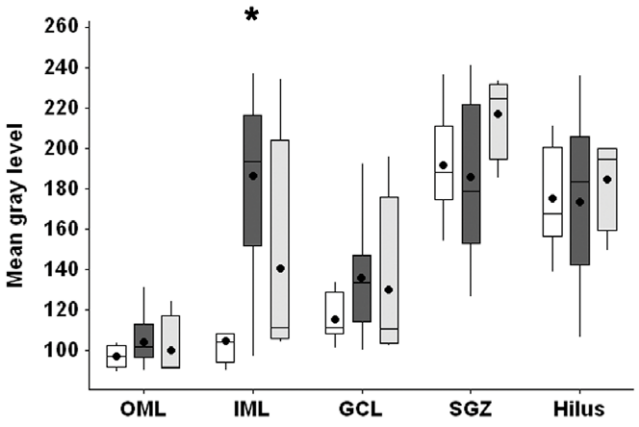

Figure 4. Vesicular zinc staining in the *Fascia dentata* of Ctrl, MTLE and TLE-TD groups. MTLE (dark gray boxplots) had increased neo-Timm staining (showed as gray level intensity), when compared to Ctrl (white boxplots), in the inner molecular layer (IML, $p<0.001$). No difference was observed between TLE-TD (light gray boxplots) and Ctrl or MTLE. The * indicate difference from Ctrl. The dark circles indicate mean.
doi:10.1371/journal.pone.0044709.g004

Correlations between MT-I/II immunoreactivity, cellular populations and vesicular Zn^{2+}

Considering all TLE patients, correlation analysis revealed that MT-I/II immunoreactivity correlated with GFAP immunoreactivity in CA4 ($r = 0.312$; $p = 0.012$; $n = 65$), CA2 ($r = 0.275$; $p = 0.038$; $n = 57$) and CA1 ($r = 0.319$; $p = 0.004$; $n = 78$) and with NeuN in CA1 ($r = -0.241$; $p = 0.034$; $n = 78$). No correlation was found between MT-I/II immunoreactivity and HLA-DR immunoreactivity or neo-Timm staining. In CA4, multiple linear regression revealed a trend to association between MT-I/II expression and GFAP immunopositivity ($r = 0.347$; $p = 0.061$, with $p = 0.753$ for NeuN, $p = 0.02$ for GFAP and $p = 0.111$ for age; $n = 53$). In CA2, multiple regression model revealed that MT expression was significantly explained by GFAP and age ($r = 0.574$; $p<0.001$, with $p = 0.533$ for NeuN, $p = 0.018$ for GFAP, $p<0.001$ for age; $n = 55$). In CA1, MT-I/II expression has a trend to be explained by increased GFAP immunoreactivity ($r = 0.364$; $p = 0.015$, with $p = 0.817$ for NeuN, $p = 0.069$ for GFAP and $p = 0.107$ for age; $n = 77$). In summary, in some hippocampal subfields (CA4, CA2, and CA1) there was a positive correlation between MT-I/II immunoreactivity and GFAP immunoreactivity. Different regressions models did not provided a best fit for any of the variables evaluated.

In TLE-TD, there was a positive correlation between NeuN and MT-I/II expression in CA4 ($r = 0.543$; $p = 0.0353$; $n = 15$). No correlation was observed between MT-I/II expression and GFAP, HLA-DR area or neo-Timm density in TLE-TD. Multiple linear

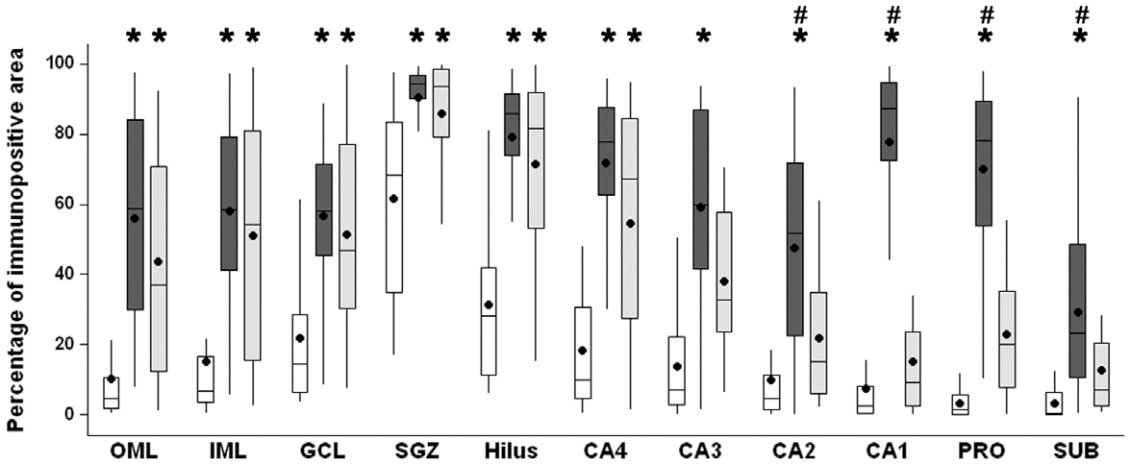

Figure 5. GFAP immunopositive area in hippocampal subfields of Ctrl, MTLE and TLE-TD groups. Compared to Ctrl (white boxplots), MTLE (dark gray boxplots) and TLE-TD (light gray boxplots) groups had increased GFAP immunoreactivity (showed as percentage of immunopositive area) in outer molecular layer (OML), inner molecular layer (IML), granule cell layer (GCL), subgranule zone (SGZ), hilus, CA4 and CA3 ($p<0.001$), and MTLE groups had increased GFAP immunopositivity in CA2, CA1, prosubiculum (PRO) and subiculum (SUB), compared to Ctrl and TLE-TD ($p<0.001$). In the subiculum (SUB), TLE-TD had increased GFAP immunoreactivity, compared to Ctrl ($p<0.001$). The * indicate difference from Ctrl and # difference from TLE-TD.
doi:10.1371/journal.pone.0044709.g005

regression model was not significant in CA4 ($r = 0.590$; $p = 0.179$; $n = 15$), but NeuN was significantly associated with MT-I/II in this region ($p = 0.046$ for NeuN, $p = 0.662$ for GFAP and $p = 0.486$ for age). For the relation between neuronal population and MT-I/II expression in CA4, the quadratic model provided a better fit, when compared to the linear model ($r^2 = 0.48$ and $p = 0.014$ for the quadratic model versus $r^2 = 0.333$ and $p = 0.019$ for the linear model)

In MTLE, MT-I/II immunoreactivity area correlated with GFAP area in CA4 (Pearson's test; $r = 0.319$; $p = 0.0241$; $n = 50$). No correlations were observed between MT expression and NeuN, HLA-DR or neo-Timm in MTLE. Multiple linear regression revealed no significance in CA4, although GFAP expression was significantly associated with MT expression ($r = 0.332$; $p = 0.175$, with $p = 0.703$ for NeuN, $p = 0.042$ for GFAP and $p = 0.269$ for age; $n = 46$). No other regression model than the linear provided a best fit for the variables evaluated.

Discussion

In the present study, we found an increased MT-I/II expression in all hippocampal subfields of MTLE patients and in the *fascia dentata* of patients with TLE-TD. In MTLE patients, MT-I/II expression correlated with astroglial population but not with neuronal population. In TLE-TD group, MT-I/II expression correlated positively with neuronal population only in CA4. In the CNS, MT-I/II are expressed mainly by astrocytes [46] and, when the tissue suffers an injury, increased MT-I/II expression is observed in astrocytes and microglias [46], [32]. In our study, an increased expression of MT-I/II was observed in astrocytes and

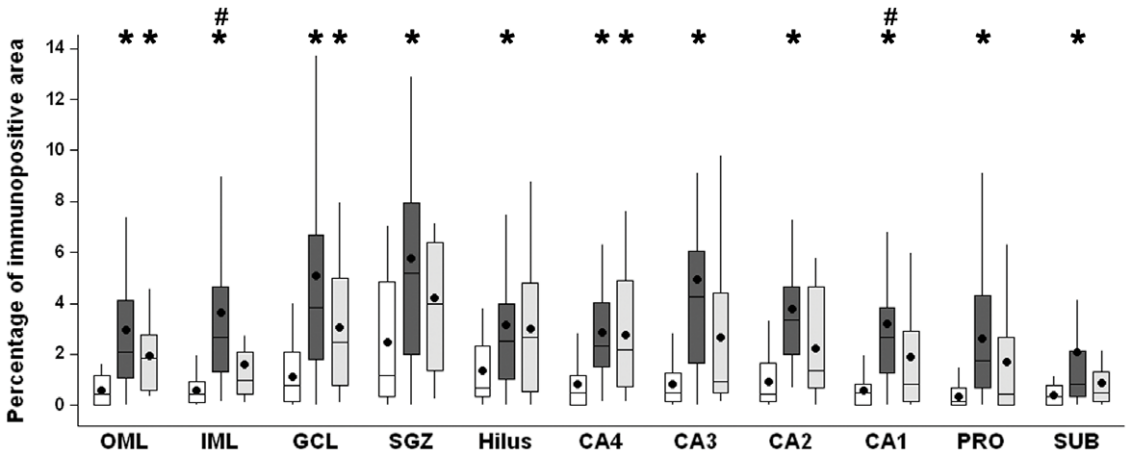

Figure 6. HLA-DR immunopositive area in hippocampal subfields of Ctrl, MTLE and TLE-TD groups. Compared to Ctrl (white boxplots), TLE groups had increased HLA-DR immunoreactivity (showed as percentage of immunopositive area) in outer molecular layer (OML), granule cell layer (GCL), CA4, and CA1 subfields ($p<0.001$). MTLE (dark gray boxplots) had increased HLA-DR immunoreactivity in inner molecular layer (IML), subgranule zone (SGZ), hilus, CA3, CA2, prosubiculum (PRO) and subiculum (SUB) ($p<0.01$). In IML, MTLE also presented increased HLA-DR immunoreactivity when compared to TLE-TD ($p<0.001$). The * indicate difference from Ctrl and # difference from TLE-TD.
doi:10.1371/journal.pone.0044709.g006

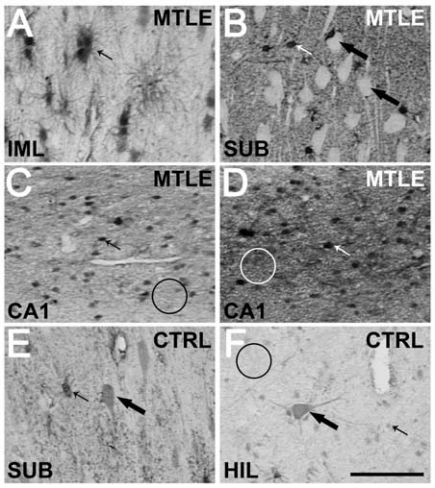

Figure 7. Representative images of MT-I/II staining in several hippocampal subfields. Almost all stained cells have astrocyte morphology (indicated by small arrows in A–F), while neurons remained unstained (white cells pointed by large arrows in B). Only in few cases from Ctrl (E and F) and in one region of one case of TLE were observed cells with neuron morphology (large arrows in E and F). No stained neuron presented the strong staining of astrocytes. In Ctrl, neuropil presented a weak staining (indicated by black circle in F). In TLE the neuropil staining level was heterogeneous, as can be seen in CA1 sections depicted in C and D (indicated by white circles). The representative images shown are from the *fascia dentate* (A), *subiculum* (B and E), CA1 (C and D) and *hilus* (F) of Ctrl (E and F) and TLE cases (A–D). Bar in F indicates 100 micrometers.
doi:10.1371/journal.pone.0044709.g007

occasionally in neurons of autopsy and TLE patients. Confocal microscopy in our TLE patients corroborated the finding that MT-I/II are expressed by astrocytes. We also observed an increased expression of MT-I/II in the neuropil of TLE patients. Studies in tissue obtained from animal models of CNS injury have shown that increased MT-I/II expression in the neuropil is most likely the result of higher release of MT-I/II from the astrocytes [47], [48]. Therefore, our data support the notion that MT-I/II changes are essentially related to astroglial population.

Gliosis is a common finding in TLE [21], [22], [23], [24] and is associated with the degree of neuronal death [22], [49], [23], [24]. Similarly with MT-I/II expression, gliosis was more intense and widespread in MTLE than in TLE-TD groups. Furthermore, correlations between the degree of astrogliosis and the expression of MT-I/II observed in TLE patients indicate that MT-I/II expression in TLE is a phenomenon associated with the astrogliosis and, consequently, with the degree of tissue damage. In agreement with this hypothesis, an association between the severity of tissue damage and the increase in MT-I/II expression has been reported in mice subjected to soman-induced SE [35].

Studies in rodents with kainic acid-induced SE showed an association between MT-I/II expression and neuronal survival. Transgenic mice over-expressing MT-I/II have reduced neuronal death, compared to wild type animals [38]. In addition, mice with reduced MT-I/II expression [36] or in knockouts for MT-I/II [37] had increased neuronal death following SE, compared to wild type mice. In our study, MT-I/II expression correlated positively with neuronal population only in CA4 of TLE-TD patients. In MTLE group, where neuronal death and MT-I/II expression are more pronounced, no correlation between neuronal death and MT-I/II was observed. These findings contradict the hypothesis that an increased MT-I/II expression could be related with

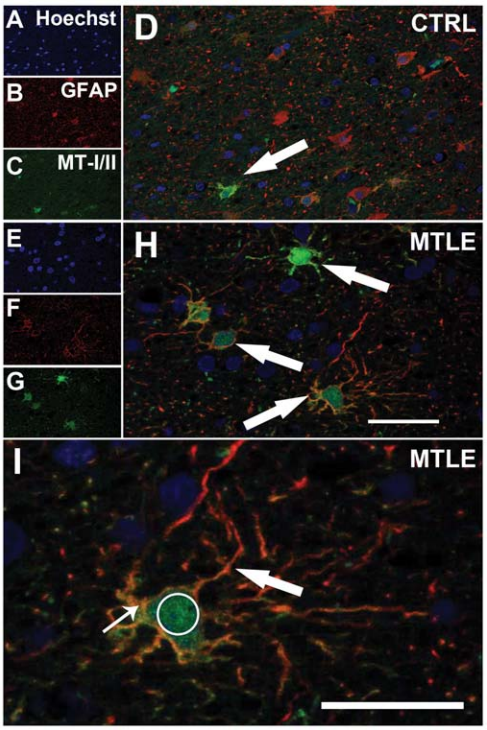

Figure 8. Confocal images of astrocytes expressing MT-I/II in Ctrl and TLE cases. TLE (E–H) patients presented more astrocytes (GFAP immunoreactive cells, red in B, F, D, H and I) expressing MT-I/II (green in C, G, D, H and I, indicated by white arrows in D and H) than Ctrl (A–D). In a detailed view of H (I), MT-I/II expression can be observed in radial branches (large arrow), soma (small arrow) and nucleus (Hoeschst 33342 staining, white circle) of astrocytes. Astrocytes are GFAP immunoreactivity) Bars in H and I indicate 50 micrometers.
doi:10.1371/journal.pone.0044709.g008

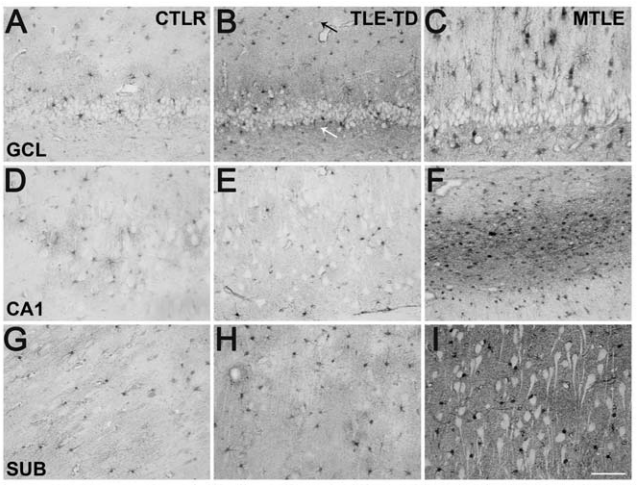

Figure 9. Representative sections of MT-I/II immunohistochemistry in hippocampal subfields from Ctrl, TLE-TD and MTLE patients. MTLE patients had widespread increase in MT-I/II when compared to Ctrl, demonstrated by increased cellular and neuropil staining in C, F and I. In TLE-TD patients, increased MT-I/II expression was observed only in the *fascia dentata* (B) outer molecular layer (small black arrow) and subgranule zone (small white arrow), the entry point of the hippocampus. The representative images shown are from the *fascia dentata* (A–C), CA1 (D–F) and subiculum (G–I). Bar in I indicates 100 micrometers.
doi:10.1371/journal.pone.0044709.g009

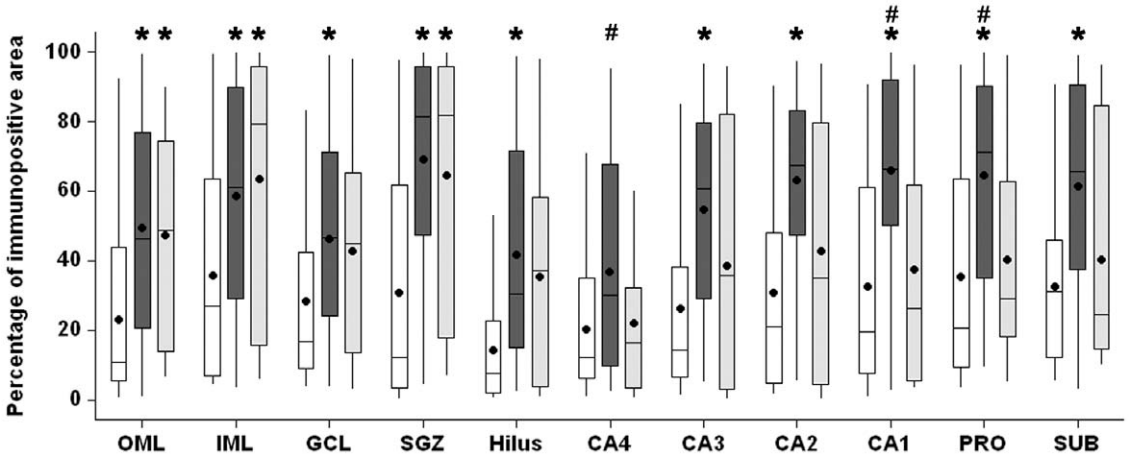

Figure 10. MT-I/II immunopositive area in hippocampal subfields of Ctrl, MTLE and TLE-TD groups. Compared to Ctrl (white boxplots), TLE groups had higher MT-I/II immunopositive area (showed as percentage of immunopositive area) in outer molecular layer (OML), inner molecular layer (IML) and subgranule zone (SGZ) ($p<0.01$). MTLE (dark gray boxplots) had increased MT-I/II immunoreactivity in granule cell layer (GCL), hilus, CA4, CA3, CA2, CA1, prosubiculum (PRO) and subiculum (SUB) ($p<0.05$), compared to Ctrl, and also in CA1 when compared to TLE-TD ($p<0.001$). The * indicate difference from Ctrl and #difference from TLE-TD.
doi:10.1371/journal.pone.0044709.g010

neuronal survival. Different mechanisms contribute to neuronal death that occurs in the hippocampus of MTLE and TLE-TD patients. In TLE-TD patients, evidence has been shown that neuronal death is a consequence of the recurrent seizures [50]. Although neuronal death in MTLE can also be caused by recurrent seizures [50], the bulk of neuronal death is rather a consequence of an initial precipitating insult (IPI), which usually occurs several years before the epilepsy onset [50], [51]. The neuronal death is also severe in MTLE, often resulting in hippocampal sclerosis, while TLE-TD patients generally have preserved neuronal density [18], [52]. In addition, data indicate that hippocampal atrophy may be determined by a strong genetic predisposition and occur in individuals who never had seizures [53]. Therefore, it is possible that the differential increase in MT-I/II expression in TLE-TD and MTLE is also the result of the different mechanisms associated with neuronal death in such epileptic syndromes.

According to other studies, MTs could also be responsible to neuronal damage and death following SE. In mice knockout for ZnT3, a protein responsible to stock Zn^{2+} in synaptic vesicles, SE increases damage in CA1 [39], [28], [29] and other cerebral regions [29], when compared to wild type mice. In these knockout mice lacking vesicular Zn^{2+}, damage in CA1 can be prevented by chelating extracellular Zn^{2+} [28], [29] or by knocking out MT-III gene [39], [29]. However, knocking out MT-III gene in mice with [54] or without vesicular Zn^{2+} [29] increases damage in CA3 after SE. Since all studies that associated MT-I/II with neuronal survival after SE studied mainly the CA3 region, where MT-III is also known to protect from damage [54], [29], one could argue that, in CA1 and other hippocampal regions, MT-I/II could cause damage, similarly to MT-III. We did not find any positive association between increased MT-I/II expression and reduced neuronal population in all hippocampal subfields. Furthermore, mice with reduced levels of MT-I/II [36] have increased damage in CA1 after SE. It is known that MT-I/II binds Zn^{2+} more

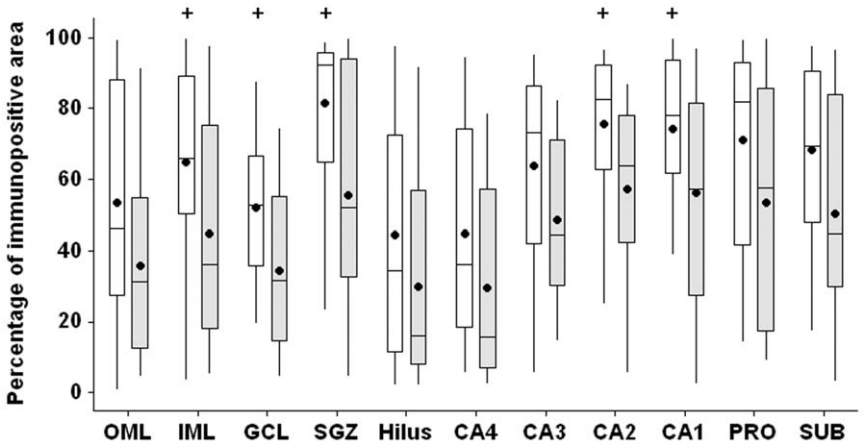

Figure 11. MT-I/II immunopositive area in MTLE patients without and with secondary generalized seizures. Patients without secondary generalization (white boxplots) present increased MT-I/II immunopositivity ($p<0.05$) in the inner molecular layer (IML), granule cell layer (GCL), subgranule zone (SGZ), CA2 and CA1, when compared with patients that present secondary generalization (light gray boxplots). The + indicates difference between the groups.
doi:10.1371/journal.pone.0044709.g011

strongly that MT-III [55], [56]. These observations make us believe that MT-I/II do not contribute to the neuronal damage observed in the hippocampus of TLE patients. Further studies must be performed to better address this issue.

Several developmental studies have indicated that MT-I/II levels increase with the age, [57], [58], [59], [60], [61], [62], [63], [64]. On the other hand, reduced MT-I/II expression has also been reported in the adult rat brain when compared to young brain [65], and no differences were observed in aged and adult brain specimens of rat [66] and calf [67]. Also, it is already known that longer epilepsy duration can increase the neuronal death observed in hippocampal sclerosis and is associated with the neuronal death in non-sclerosis cases [50]. Therefore, we must also account for age and epilepsy duration as factors for the changes observed in MT-I/II expression. We did not see relation between epilepsy duration and MT expression in our multivariate analysis. However, in some regions, age at evaluation was significantly associated with MT-I/II expression. For example, in CA2 of all TLE patients and in CA4 of TLE-TD age at evaluation predicted MT-I/II expression. Although our findings indicate that age can contribute to the increased MT-I/II expression observed in TLE, the pathological changes associated to the epileptic condition (i.e., gliosis and neuronal death) are still the main factors related to the increased MT-I/II expression in the hippocampus of TLE patients.

Reorganization of vesicular Zn^{2+} in the hippocampus is often observed in TLE [19], [20], and Zn^{2+} can trigger MT-I/II expression [59]. Then, it is also important to consider the effect of the Zn^{2+} pool over MT-I/II expression. In agreement with other studies [68], [69], [19], we only observed significant increase in vesicular Zn^{2+} in the inner molecular layer of MTLE patients. No correlation was observed between MT-I/II expression and vesicular Zn^{2+} in our TLE cases. This does not exclude an association between MT-I/II expression and Zn^{2+}, provided that only 10% of all Zn^{2+} in the brain is located in vesicles [70], [7] and only a small fraction of the Zn^{2+} released during neurotransmission will reach the astrocytes to induce MT-I/II expression.

Data have shown that the increased MT-I/II immunoreactivity observed in animal models of TLE can also be a factor associated with the seizure generation process. Transgenic mice over-expressing MT-I, have increased seizure duration, a tendency to reduced latency, but similar number of seizures after kainic acid administration [38]. Since MT-I/II act chelating free Zn^{2+} [31], [14] and Zn^{2+} chelation increases tissue excitability and facilitates seizure generation [71], excessive MT-I/II levels can reduce free Zn^{2+} in the synaptic cleft, increasing neuronal excitability and affecting seizure generation. Our data showed a similar frequency of seizure between MTLE and TLE-TD patients. In agreement with previous studies, we found no correlation between seizure frequency and MT-I/II expression in TLE [38].

In MTLE, we found increased levels of MT-I/II expression in patients without SGS, when compared with those with SGS. This could indicate that MT-I/II expression is associated with different seizure spread patterns from the epileptogenic hippocampus to other brain regions. It is important to point out that no difference in neurons or glial cells was observed between MTLE with and without SGS. Studies from different groups also observed no association between changes in the hippocampus and SGS [72], [73], [74]. These observations suggest that the increased MT-I/II expression in patients without SGS is not an effect of gliosis, but it is independently associated with SGS. Further studies with animal models of TLE should evaluate more closely the relationship between MT-I/II expression and seizure susceptibility.

The differential pattern of increase in MT-I/II expression in MTLE and TLE-TD patients may also be associated with the site of seizure generation. Seizures are known to induce MT-I/II expression in the epileptic hippocampus [75]. In MTLE patients, where MT-I/II increase was widespread, most focal seizures are generated within the hippocampus [76]. In TLE-TD, the seizures are generally generated in the cerebral cortex surrounding the tumor or in the cortical dysplasia and hence propagate to the hippocampus [18], [77], [78]. The main area of input entry in the hippocampus is the molecular layer of the *fascia dentata* [10], where increased MT-I/II expression was observed in the TLE-TD patients of our study.

Some limitations of our study must be pointed out. So far, studies about MT-I/II expression in animal models of TLE only evaluated the acute period following SE. Considering that our study was performed in patients with chronic epilepsy, it is difficult to establish comparisons between human and animal data. Besides, the reduced number of patients in the TLE-TD group can be the reason why only in one hippocampal subfields the neuronal density correlated with MT-I/II expression. The lack of correlation between seizure frequency and MT-I/II expression does not exclude an association between seizures and MT-I/II expression. Other seizure characteristics, such as seizure duration and time between the last seizure and the surgery, could better correlate with MT-I/II expression than isolated seizure frequency.

Finally, our study may have translational implications in the future. The role of MTs in antiinflamatory response, neurotrophic factor expression, and protection against ROS and heavy metals make those proteins interesting for clinical applications. Studies have shown that EmtinB, a syntethic peptide that mimics the actions of MTs, attenuates kainic acid-induced seizures and protects neurons from excitotoxic death [34]. Further studies with EmtinB and MTs in acute and chronic models of epilepsy might assess, in more detail, the role of these proteins in neuronal survival and seizure susceptibility.

In summary, our data indicate that increased MT-I/II expression is a plastic alteration of chronic TLE, primarily related to the astrogliosis, a common finding in chronic TLE. In opposition to other studies, MT-I/II expression was not associated with significant neuronal survival in TLE. Nevertheless, our findings suggest that increased MT-I/II expression may contribute to the control of the brain hyperexcitability.

Supporting Information

Figure S1 Representative images of immunohistochemistries in the temporal cortex from a MTLE patient. After surgery, tissue fragments were maintained in saline solution during 1 hour (A, F, K and P), 4 hours (B, G, L and Q) and 8 hour (C, H, M and R) prior to fixation in formaline. Note that no difference can be seen regardless of waiting time prior to fixation for MT-I/II (A–C), GFAP (F–H), HLA-DR (K–M) and NeuN (P–R) immunoreactivities. Statistical analyses did not revealed difference in immunopositive area (D, I, N and S) or gray level (E, J, O and T) between tissues fixed after 1 (white boxplot), 2 (very light gray boxplot), 4 (light gray boxplot), 6 (medium gray boxplot) or 8 (dark gray boxplot) hours post surgery for MT-I/II (D and E), GFAP (I and J), HLA-DR (N and O) or NeuN (S and T). Bar in R indicates 100 micrometers.
(TIF)

Author Contributions

Conceived and designed the experiments: JEPS OYGA JPL. Performed the experiments: JEPS TRV LK RCS. Analyzed the data: JEPS OYGA.

Contributed reagents/materials/analysis tools: JEPS LK JAA CGC RCS LNS JPL. Wrote the paper: JEPS TRV JPL.

References

1. Peters S, Koh J, Choi DW (1987) Zinc selectively blocks the action of N-methyl-D-aspartate on cortical neurons. Science 236 (4801): 589–593.
2. Westbrook GL, Mayer ML (1987) Micromolar concentrations of Zn2+ antagonize NMDA and GABA responses of hippocampal neurons. Nature 328 (6131): 640–643.
3. Rassendren FA, Lory P, Pin JP, Nargeot J (1990) Zinc has opposite effects on NMDA and non-NMDA receptors expressed in Xenopus oocytes. Neuron 4 (5): 733–740.
4. Haug FMS (1967) Electron microscopic localization of the zinc in hippocampal mossy fiber synapses by a modified sulphide silver procedure. Histochemie 8 : 355–368.
5. Frederickson CJ, Hernandez MD, McGinty JF (1989) Translocation of zinc may contribute to seizure-induced death of neurons. Brain Res 480 (1–2): 317–321.
6. Perez-Clausell J (1996) Distribution of terminal fields stained for zinc in the neocortex of the rat. J Chem Neuroanat 11 (2): 99–111.
7. Frederickson CJ, Suh SW, Silva D, Frederickson CJ, Thompson RB (2000) Importance of zinc in the central nervous system: the zinc-containing neuron. J Nutr 130 (5S Suppl): 1471S–1483S.
8. Brown CE, Dyck RH (2004) Distribution of zincergic neurons in the mouse forebrain. J Comp Neurol 479 (2): 156–167.
9. Takeda A, Itoh H, Tamano H, Oku N (2006) Responsiveness to kainate in young rats after 2-week zinc deprivation. Biometals 19 (5): 565–572.
10. Amaral D, Lavenex P (2006) Hippocampal Neuroanatomy. The Hippocampus Book: Oxford University Press. pp. 37–114
11. Mathern GW, Babb TL, Leite JP, Pretorius K, Yeoman KM, et al. (1996) The pathogenic and progressive features of chronic human hippocampal epilepsy. Epilepsy Res 26 (1): 151–161.
12. Pitkanen A (2002) Efficacy of current antiepileptics to prevent neurodegeneration in epilepsy models. Epilepsy Res 50 (1–2): 141–160.
13. Weiss JH, Sensi SL, Koh JY (2000) Zn(2+): a novel ionic mediator of neural injury in brain disease. Trends Pharmacol Sci 21 (10): 395–401.
14. Colvin RA, Fontaine CP, Laskowski M, Thomas D (2003) Zn2+ transporters and Zn2+ homeostasis in neurons. Eur J Pharmacol 479 (1–3): 171–185.
15. Kim EY, Koh JY, Kim YH, Sohn S, Joe E, et al. (1999) Zn2+ entry produces oxidative neuronal necrosis in cortical cell cultures. Eur J Neurosci 11 (1): 327–334.
16. Treiber C (2005) Metals on the brain. Sci Aging Knowledge Environ 2005 (36): e27–
17. Frederickson CJ, Koh JY, Bush AI (2005) The neurobiology of zinc in health and disease. Nat Rev Neurosci 6 (6): 449–462.
18. Babb TL, Brown WJ, Pretorius J, Davenport C, Lieb JP, et al. (1984) Temporal lobe volumetric cell densities in temporal lobe epilepsy. Epilepsia 25 (6): 729–740.
19. Babb TL, Kupfer WR, Pretorius JK, Crandall PH, Levesque MF (1991) Synaptic reorganization by mossy fibers in human epileptic fascia dentata. Neuroscience 42 (2): 351–363.
20. Mathern GW, Leite JP, Babb TL, Pretorius JK, Kuhlman PA, et al. (1996) Aberrant hippocampal mossy fiber sprouting correlates with greater NMDAR2 receptor staining. Neuroreport 7 (5): 1029–1035.
21. Salanova V, Markand O, Worth R, Garg B, Patel H, et al. (1999) Presurgical evaluation and surgical outcome of temporal lobe epilepsy. Pediatr Neurol 20 (3): 179–184.
22. Proper EA, Jansen GH, van Veelen CW, van Rijen PC, Gispen WH, et al. (2001) A grading system for hippocampal sclerosis based on the degree of hippocampal mossy fiber sprouting. Acta Neuropathol (Berl) 101 (4): 405–409.
23. Swartz BE, Houser CR, Tomiyasu U, Walsh GO, DeSalles A, et al. (2006) Hippocampal cell loss in posttraumatic human epilepsy. Epilepsia 47 (8): 1373–1382.
24. Prayson RA, Yoder BJ (2007) Clinicopathologic findings in mesial temporal sclerosis treated with gamma knife radiotherapy. Ann Diagn Pathol 11 (1): 22–26.
25. Sutula T, Cascino G, Cavazos J, Parada I, Ramirez L (1989) Mossy fiber synaptic reorganization in the epileptic human temporal lobe. Ann Neurol 26 (3): 321–330.
26. Sensi SL, Ton-That D, Sullivan PG, Jonas EA, Gee KR, et al. (2003) Modulation of mitochondrial function by endogenous Zn2+ pools. Proc Natl Acad Sci U S A 100 (10): 6157–6162.
27. Sensi SL, Paoletti P, Koh JY, Aizenman E, Bush AI, et al. (2011) The neurophysiology and pathology of brain zinc. J Neurosci 31 (45): 16076–16085.
28. Lee JY, Cole TB, Palmiter RD, Koh JY (2000) Accumulation of zinc in degenerating hippocampal neurons of ZnT3-null mice after seizures: evidence against synaptic vesicle origin. J Neurosci 20 (11): RC79–
29. Lee JY, Kim JH, Palmiter RD, Koh JY (2003) Zinc released from metallothionein-iii may contribute to hippocampal CA1 and thalamic neuronal death following acute brain injury. Exp Neurol 184 (1): 337–347.
30. Kille P, Hemmings A, Lunney EA (1994) Memories of metallothioneis. Biochim Biophys Acta 1205 : 151–161.
31. Aschner M, Cherian MG, Klaassen CD, Palmiter RD, Erickson JC, et al. (1997) Metallothioneins in brain–the role in physiology and pathology. Toxicol Appl Pharmacol 142 (2): 229–242.
32. Wiese L, Kurtzhals JA, Penkowa M (2006) Neuronal apoptosis, metallothionein expression and proinflammatory responses during cerebral malaria in mice. Exp Neurol 200 (1): 216–226.
33. Ebadi M, Brown-Borg H, El RH, Singh BB, Garrett S, et al. (2005) Metallothionein-mediated neuroprotection in genetically engineered mouse models of Parkinson's disease. Brain Res Mol Brain Res 134 (1): 67–75.
34. Sonn K, Pankratova S, Korshunova I, Zharkovsky A, Bock E, et al. (2010) A metallothionein mimetic peptide protects neurons against kainic acid-induced excitotoxicity. J Neurosci Res 88 (5): 1074–1082.
35. Pazdernik TL, Emerson MR, Cross R, Nelson SR, Samson FE (2001) Soman-induced seizures: limbic activity, oxidative stress and neuroprotective proteins. J Appl Toxicol 21 Suppl 1 : S87–S94.
36. Penkowa M, Molinero A, Carrasco J, Hidalgo J (2001) Interleukin-6 deficiency reduces the brain inflammatory response and increases oxidative stress and neurodegeneration after kainic acid-induced seizures. Neuroscience 102 (4): 805–818.
37. Carrasco J, Penkowa M, Hadberg H, Molinero A, Hidalgo J (2000) Enhanced seizures and hippocampal neurodegeneration following kainic acid-induced seizures in metallothionein-I+II-deficient mice. Eur J Neurosci 12 (7): 2311–2322.
38. Penkowa M, Florit S, Giralt M, Quintana A, Molinero A, et al. (2005) Metallothionein reduces central nervous system inflammation, neurodegeneration, and cell death following kainic acid-induced epileptic seizures. J Neurosci Res 79 (4): 522–534.
39. Cole TB, Robbins CA, Wenzel HJ, Schwartzkroin PA, Palmiter RD (2000) Seizures and neuronal damage in mice lacking vesicular zinc. Epilepsy Res 39 (2): 153–169.
40. Leite JP, Terra-Bustamante VC, Fernandes RM, Santos AC, Chimelli L, et al. (2000) Calcified neurocysticercotic lesions and postsurgery seizure control in temporal lobe epilepsy. Neurology 55 (10): 1485–1491.
41. Berg AT (2009) Identification of pharmacoresistant epilepsy. Neurol Clin 27 (4): 1003–1013.
42. Mathern GW, Leite JP, Pretorius JK, Quinn B, Peacock WJ, et al. (1994) Children with severe epilepsy: evidence of hippocampal neuron losses and aberrant mossy fiber sprouting during postnatal granule cell migration and differentiation. Brain Res Dev Brain Res 78 (1): 70–80.
43. Kandratavicius L, Hallak JE, Young LT, Assirati JA, Carlotti CG Jr, et al. (2012) Differential aberrant sprouting in temporal lobe epilepsy with psychiatric comorbidities. Psychiatry Res 195 (3): 144–150.
44. Lorente de Nó R (1934) Studies on the structure of the cerebral cortex. II. Continuation of the study of the ammoniac system. Journal of Psychologie und Neurologie 45 : 113–177.
45. Abercrombie M (1946) Estimation of nuclear population from microtome sections. Anat Rec 94 : 239–147.
46. Hidalgo J (2004) Metallothioneins and Brain Injury: What Transgenic Mice Tell Us. Environ Health Prev Med : 87–94.
47. Chung RS, West AK (2004) A role for extracellular metallothioneins in CNS injury and repair. Neuroscience 123 (3): 595–599.
48. Chung RS, Penkowa M, Dittmann J, King CE, Bartlett C, et al. (2008) Redefining the role of metallothionein within the injured brain: extracellular metallothioneins play an important role in the astrocyte-neuron response to injury. J Biol Chem 283 (22): 15349–15358.
49. Crespel A, Coubes P, Rousset MC, Brana C, Rougier A, et al. (2002) Inflammatory reactions in human medial temporal lobe epilepsy with hippocampal sclerosis. Brain Res 952 (2): 159–169.
50. Mathern GW, Adelson PD, Cahan LD, Leite JP (2002) Hippocampal neuron damage in human epilepsy: Meyer's hypothesis revised. Prog Brain Res 135 : 237–251.
51. Pitkanen A, Sutula TP (2002) Is epilepsy a progressive disorder? Prospects for new therapeutic approaches in temporal-lobe epilepsy. Lancet Neurol 1 (3): 173–181.
52. Kim JH, Guimaraes PO, Shen MY, Masukawa LM, Spencer DD (1990) Hippocampal neuronal density in temporal lobe epilepsy with and without gliomas. Acta Neuropathol 80 (1): 41–45.
53. Kobayashi E, Li LM, Lopes-Cendes I, Cendes F (2002) Magnetic resonance imaging evidence of hippocampal sclerosis in asymptomatic, first-degree relatives of patients with familial mesial temporal lobe epilepsy. Arch Neurol 59 (12): 1891–1894.
54. Erickson JC, Hollopeter G, Thomas SA, Froelick GJ, Palmiter RD (1997) Disruption of the metallothionein-III gene in mice: analysis of brain zinc, behavior, and neuron vulnerability to metals, aging, and seizures. J Neurosci 17 (4): 1271–1281.
55. Frederickson CJ, Maret W, Cuajungco MP (2004) Zinc and excitotoxic brain injury: a new model. Neuroscientist 10 (1): 18–25.

56. Palumaa P, Tammiste I, Kruusel K, Kangur L, Jornvall H, et al. (2005) Metal binding of metallothionein-3 versus metallothionein-2: lower affinity and higher plasticity. Biochim Biophys Acta 1747 (2): 205–211.
57. Natale JE, Knight JB, Cheng Y, Rome JE, Gallo V (2004) Metallothionein I and II mitigate age-dependent secondary brain injury. J Neurosci Res 78 (3): 303–314.
58. Waalkes MP, Klaassen CD (1984) Postnatal ontogeny of metallothionein in various organs of the rat. Toxicol Appl Pharmacol 74 (3): 314–320.
59. Ebadi M, Iversen PL, Hao R, Cerutis DR, Rojas P, et al. (1995) Expression and Regulation of Brain Metallothionein. Neurochem Int 27 (1): 1–22.
60. Suzuki K, Nakajima K, Otaki N, Kimura M (1994) Metallothionein in developing human brain. Biol Signals 3 (4): 188–192.
61. Marijic VF, Raspor B (2006) Age- and tissue-dependent metallothionein and cytosolic metal distribution in a native Mediterranean fish, Mullus barbatus, from the Eastern Adriatic Sea. Comp Biochem Physiol C Toxicol Pharmacol 143 (4): 382–387.
62. Lu T, Pan Y, Kao SY, Li C, Kohane I, et al. (2004) Gene regulation and DNA damage in the ageing human brain. Nature 429 (6994): 883–891.
63. Suzuki K, Nakajima K, Kawaharada U, Uehara K, Hara F, et al. (1992) Metallothionein in the human brain. Acta Histochem Cytochem 25 (6): 617–622.
64. Mocchegiani E, Bertoni-Freddari C, Marcellini F, Malavolta M (2005) Brain, aging and neurodegeneration: role of zinc ion availability. Prog Neurobiol 75 (6): 367–390.
65. Nishimura N, Nishimura H, Ghaffar A, Tohyama C (1992) Localization of metallothionein in the brain of rat and mouse. J Histochem Cytochem 40 (2): 309–315.
66. Gomi F, Nakano S, Uchida Y (2005) Tolerance of aged rat brains to mild hyperoxia: possible involvement of higher GIF content. Brain Res 1033 (1): 113–116.
67. Zatta P, Drago D, Zambenedetti P, Bolognin S, Nogara E, et al. (2008) Accumulation of copper and other metal ions, and metallothionein I/II expression in the bovine brain as a function of aging. J Chem Neuroanat 36 (1): 1–5.
68. Mathern GW, Pretorius JK, Babb TL, Quinn B (1995) Unilateral hippocampal mossy fiber sprouting and bilateral asymmetric neuron loss with episodic postictal psychosis. J Neurosurg 82 (2): 228–233.
69. Mathern GW, Pretorius JK, Babb TL (1995) Quantified patterns of mossy fiber sprouting and neuron densities in hippocampal and lesional seizures. J Neurosurg 82 (2): 211–219.
70. Frederickson CJ, Hernandez MD, Goik SA, Morton JD, McGinty JF (1988) Loss of zinc staining from hippocampal mossy fibers during kainic acid induced seizures: a histofluorescence study. Brain Res 446 (2): 383–386.
71. Dominguez MI, Blasco-Ibanez JM, Crespo C, Nacher J, Marques-Mari AI, et al. (2006) Neural overexcitation and implication of NMDA and AMPA receptors in a mouse model of temporal lobe epilepsy implying zinc chelation. Epilepsia 47 (5): 887–899.
72. Bernasconi N, Natsume J, Bernasconi A (2005) Progression in temporal lobe epilepsy: differential atrophy in mesial temporal structures. Neurology 65 (2): 223–228.
73. Szabo CA, Lancaster JL, Lee S, Xiong JH, Cook C, et al. (2006) MR imaging volumetry of subcortical structures and cerebellar hemispheres in temporal lobe epilepsy. AJNR Am J Neuroradiol 27 (10): 2155–2160.
74. O'Dwyer R, Silva Cunha JP, Vollmar C, Mauerer C, Feddersen B, et al. (2007) Lateralizing significance of quantitative analysis of head movements before secondary generalization of seizures of patients with temporal lobe epilepsy. Epilepsia 48 (3): 524–530.
75. Montpied P, de Bock F, Baldy-Moulinier M, Rondouin G (1998) Alterations of metallothionein II and apolipoprotein J mRNA levels in kainate-treated rats. Neuroreport 9 (1): 79–83.
76. Wennberg R, Arruda F, Quesney LF, Olivier A (2002) Preeminence of extrahippocampal structures in the generation of mesial temporal seizures: evidence from human depth electrode recordings. Epilepsia 43 (7): 716–726.
77. Engel J Jr (1996) Introduction to temporal lobe epilepsy. Epilepsy Res 26 (1): 141–150.
78. Surges R, Schulze-Bonhage A, Altenmuller DM (2008) Hippocampal involvement in secondarily generalised seizures of extrahippocampal origin. J Neurol Neurosurg Psychiatry 79 (8): 924–929.